Optimizing regenerative braking on electric vehicles using a model-based algorithm in the antilock braking system

Agung Prijo Budijono[1,2], I Nyoman Sutantra[2], Agus Sigit Pramono[2]
[1]Department of Mechanical Engineering, Faculty of Engineering, Universitas Negeri Surabaya, Surabaya, Indonesia
[2]Department of Mechanical Engineering, Faculty of Industrial Technology, Institut Teknologi Sepuluh Nopember, Surabaya, Indonesia

Article Info

Article history:

Received May 19, 2022
Revised Oct 21, 2022
Accepted Nov 2, 2022

Keywords:

Antilock braking system
Electric vehicles
Friction frequency
Harvesting energy
Model-based algorithms
Regenerative braking

ABSTRACT

The regenerative braking effectiveness of electric vehicles (EVs), with 8-25% range, requires designers to produce better braking systems. The antilock braking system (ABS) was chosen because it offers various advantages, such as enhanced safety considerations, vehicle maneuverability, and so on. The measurement findings revealed that ABS took longer to stop the wheels with the same wheel rotation speed. Because of the lesser differentiation of magnetic flux to time, it created lower induced emf in the generator. ABS 50 Hz performance was 19.5% at 4500 pm, whereas hydraulic brake performance was 21% at the same speed. ABS used model-based algorithms (MBAs) to boost the friction frequency with the wheels from 10 to 50 Hz. As the frequency increased, the ABS graph approached the hydraulic graph, and the ABS performance improved. Although ABS loses to hydraulics in stopping wheel rotation, it gains in saved energy and battery temperature. Longer wheel stop-times allow the rotational kinetic energy of the wheel more time to be converted into electricity.

Corresponding Author:

Agung Prijo Budijono
Department of Mechanical Engineering, Faculty of Engineering, Universitas Negeri Surabaya
Unesa Ketintang Campus, Jalan Ketintang, Surabaya 60231, Indonesia
Email: agungbudijono@unesa.ac.id

1. INTRODUCTION

Electric vehicles (EVs) are a viable option for reducing air pollution and fuel consumption caused by combustion engines [1]. EVs are also more efficient than combustion engines since they recuperate energy during operation. Regenerative braking is one method of restoring [2]. Regenerative braking uses kinetic energy from the braking process, in which the wheels continue to rotate even after braking has been applied. This kinetic energy is turned into electricity, which is then stored in batteries. As a result, regenerative braking is constrained by vehicle speed and battery state of charge (SOC) [3]. Allocating braking torque also takes into account vehicle stability and energy recovery to the greatest extent practicable.

Many lives have been lost as a result of automobile accidents on the highway caused by braking. The antilock brake system (ABS) and the traction control system (TCS) may both be modified on the vehicle's dynamic control [4]. ABS gives a vehicle stability solution. During the braking procedure, the driver retains control of the car. ABS is consistent because it uses an algorithm to control hydraulic pressure in the brakes, which is classified into two types: model-based algorithms (MBAs) and rule-based algorithms (RBAs) [5]. The MBA mathematically models the braking process and necessitates a significant amount of data input. It is more precise. Meanwhile, RBA bases its algorithm on the control action's essential factors. It is less complicated.

In this study, we used powertrain components (induction motor, generator, and battery) to model the application of regenerative braking in EVs. Accuracy in powertrain component location will improve the vehicle's NVH (noise, vibration, and harshness) behavior [6]. To provide the same torque, the induction motor rotated the driving wheel (DW) through the pulley in a one-to-one ratio. Because the gears had a two-to-one ratio, the energy collected (ECW) shaft had twice the speed of the DW axle, as indicated in Figure 1. The different axles enabled more steady rotation [7], while the double speed meant greater fluxes for the generator [8]. Section 2 of the paper describes how regenerative braking works on the antilock braking system (ABS). Section 3 covers the components of this study's regenerative braking mechanism. Section 4 presents the results of the measurements and speed computations. Section 5 concludes with the optimum regenerative braking conclusion.

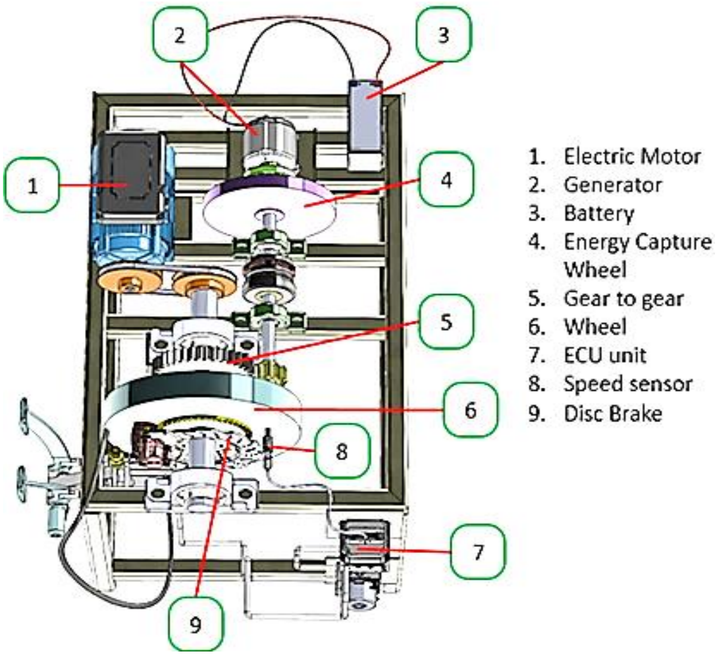

Figure 1. Experimental configuration

2. REGENERATIVE BRAKING

EVs are closely related to regenerative braking because the energy lost due to the braking process ranges from 30% to 50% [9]. Regenerative braking can provide recovery of 8% to 25% [10]. This range challenges designers to create high-efficiency regenerative braking. Frictional braking system (FBS) and regenerative braking system (RBS) are the two braking systems on current EVs. FBS is a conventional system. RBS breaks the motor and converts the kinetic energy into electricity to charge the battery. In addition, structural reconstruction is required in regenerative braking to separate pedal force and brake pressure [11]. It is usually called a brake-by-wire system, and braking effectiveness increases.

Accurate braking required real-time identification of road conditions [12]. It would be used as a reference in determining the braking torque. The ABS controlled this torque to achieve wheel-slip based on the wheel-deceleration approach. Also, ABS used a motor to drive the actuator arm [13]. It provided controllable torque all the time. This control used the Kalman filter algorithm in real-time, where the wheel speed estimation was processed based on the signals obtained by the wheel-speed sensor [14]. This algorithm was also produced to increase the precision in speed estimation on composite braking systems.

Cuma *et al.* [15] introduced the one-pedal driving (OPD) algorithm could increase the percentage of energy recovery on electric buses. This test was carried out on an urban traffic route and a constant speed test. As a result, the OPD value reached 40%, while the standard drive mode was only 34% for urban traffic. Similarly, the OPD touched 31%, whereas the drive mode was around 13% for the constant speed test. Zhou and Huang [16] presented the algorithm also increased the percentage of regenerative braking in energy distribution for some controls on electric vehicles with a two-speed transmission. Figure 2 shows that result.

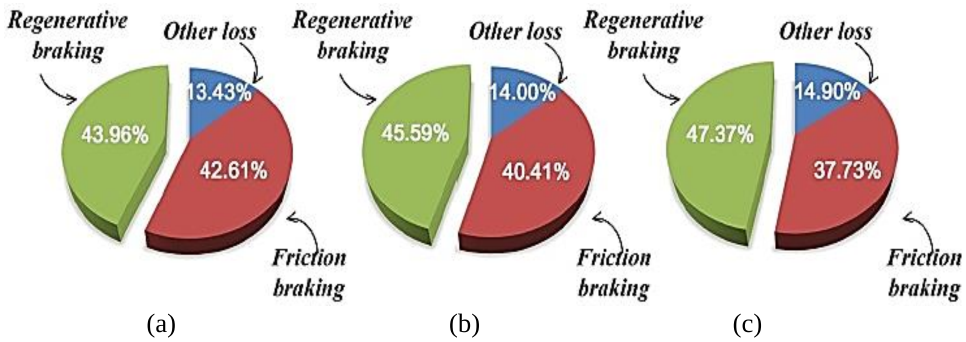

Figure 2. Energy distribution during moderate braking: (a) baseline control, (b) dynamic control, and (c) proposed control

3. EXPERIMENTAL COMPONENTS

3.1. Powertrain

Current technological developments force people to produce motors with specifications of high speed, high capacity, high accuracy, and high efficiency. One effort to fulfil this is to combine two or more eccentric motors [17]. The result satisfies the above conditions, but it causes vibration problems. The use of multiple shafts can solve this problem. The addition of a pulley to connect the two axles minimizes the resulting vibration. Table 1 shows the specifications of the DC induction motor used in this study.

The relationship between power, torque and speed of the motor is as follows:

$$P = \frac{2\pi nT}{60} \tag{1}$$

Where *P* is power in Watt, *n* is the speed in rpm, and *T* is torque in N.m.

A motor-driven generator is a converter of kinetic energy into electrical energy. It requires a high magnetic flux to produce a stable electric current. It could not be provided by regenerative braking because the rotation of the shaft in the braking process decreased. High flux concentrations can be created by chamfering the ends of the stator feet [18]. Another way is to increase the rotational speed of the drive shaft by giving the gear ratio. The DC generator specifications are listed in Table 2.

The induced emf and the electric current generated by the generator are presented by (2) and (3), respectively.

$$\varepsilon_{ind} = -N\frac{d\phi}{dt} \tag{2}$$

$$I_{ind} = \frac{\varepsilon_{ind}}{R} \tag{3}$$

Where ε_{avg} is the induced emf in Volts, *N* is the number of windings, ϕ is the magnetic flux, *t* is the time, I_{ind} is the induced current in Ampere, and *R* is the resistance in Ω. In (2) correct. It can be proven as follows: The braking time is short compared to the flux generated by the rotation of the shaft. Flux changes with time can be said to be rapid, and the flux function can be derived with time.

Battery storage capacity is the next obstacle that can reduce efficiency. The problem that is often experienced was the occurrence of electrical overloading (EOL) during the filling process on the track. One of the causes was excess torque on the rotating shaft of the generator, and no recovery phase was available [19]. Therefore, there is a need for interaction between charge control, on-track power management, and mitigating battery power degradation [20]. It can increase efficiency as desired.

Table 1. Motor DC specifications

Specifications	Value	Unit
Voltage	48	Volt
Power	350	Watt
Current	9.4	Ampere
Load (max)	350	kg
Torque	1.5–7.5	N.m
Speed	500 – 2750	rpm
Ratio	1:5	-

Table 2. Generator DC specifications

Specifications	Value	Unit
Voltage	24	Volt
Power	250	Watt
Current	16.4	Ampere
Load (max)	350	kg
Speed rate	2700	rpm

3.2. Antilock braking system (ABS)

ABS is an active safety system for vehicles. The firm factors that affect its safety were the tire design parameters and operating conditions on the tire force characteristics [21]. It can maintain the slip ratio at some value to avoid locking the tires, thereby maximizing friction potential [22]. Friction in the braking process can be used to charge the battery instead of being discharged as heat [23]. Vehicle energy is lost about 20 to 70% during braking [24]. Modeling and simulation are carried out to create performance and safety in automotive [25].

Slip ratio is a determining parameter in ABS using MBA. Figure 3 is the result of previous research, which shows the relationship between braking force and slip ratio based on road conditions. Road conditions were a complex factor to predict. It was only approachable. F_x is the frictional force in N, and κ is the slip ratio.

ABS needs to work at the maximum coefficient of friction and optimal slip ratio (λ_p) to avoid wheel locking (λ=1), maintain driving ability and vehicle stability, and improve braking performance in deceleration and stopping distance [5]. Figure 4 presents this relationship with the normalized braking force/coefficient of friction versus slip ratio. ABS is expected to work in the desired operation region, as shown in Figure 4.

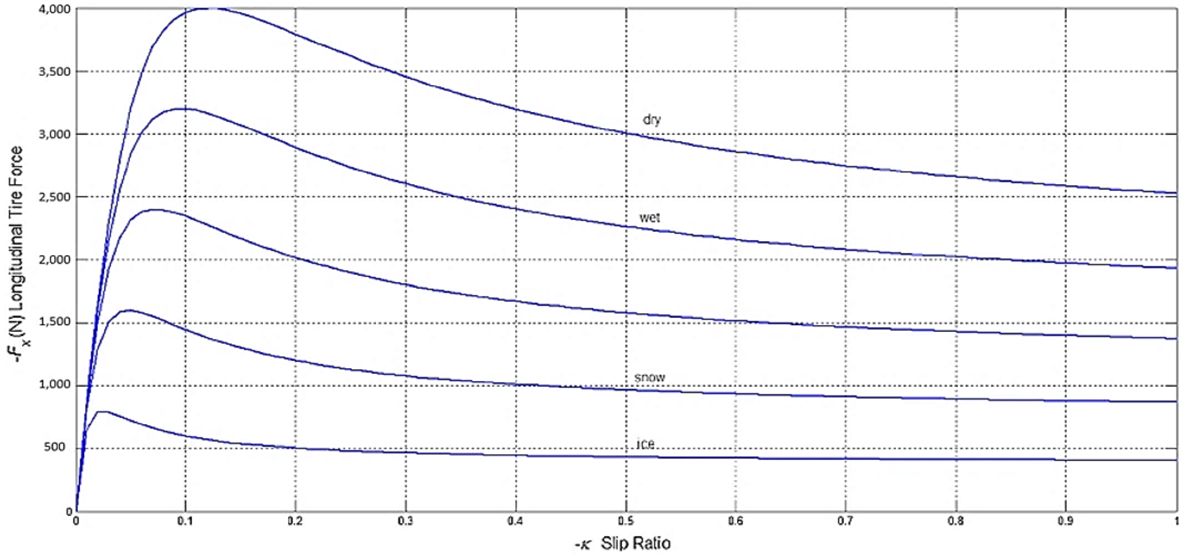

Figure 3. The relationship between tire friction and slip ratio for some road conditions

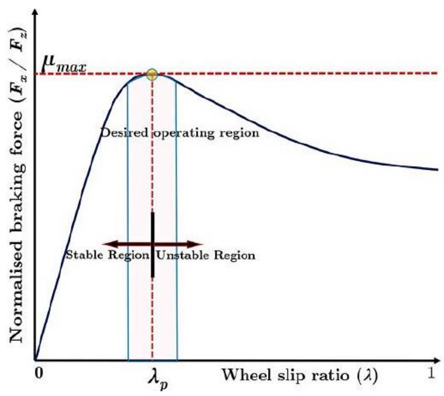

Figure 4. Normalized braking force (μ) versus slip ratio (λ) curve

According to [26], braking and traction forces will decrease with increasing speed. The traction force had a higher value than the frictional resistance force, even though it escalated with increasing rotation. Figure 5(a) shows the maximum traction and Figure 5(b) shows the maximum braking on a commercial train. The self-optimization algorithm of frictional force and slip ratio produced an ABS signal graph with distance (S), velocity ($\dot{S}$), and a positive constant (γ) as parameters, as shown in Figure 6(a) for positive speed and

Figure 6(b) for the negative one. It applied to both positive and negative friction forces (relative to vehicle motion). This signal also expressed the form of the induced emf signal in the generator as they were connected [27]. Also, [28] indicated the same signal form in the energy recovery of electric vehicles using the LQR control of interleaved double dual boost (IDDB) converter.

The positive direction of the graph above shows the direction of motion of the vehicle, while the negative direction shows the direction of the braking force. The simulation in Figure 6 produces points P_1 or P_2, which will move along the curve to point P_3 or P_4, respectively, as shown in Figure 7 [22]. Points P_3 and P_4 are points close to the optimal slip ratio and maximum friction coefficient. When crossing points P_1 or P_2, a gradient $dF_x(\kappa)/d\kappa$ is either positive or negative.

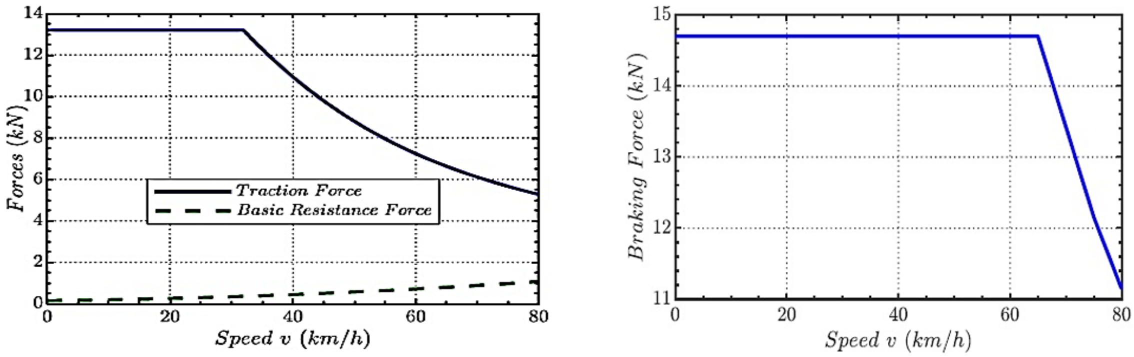

Figure 5. The results of measuring these forces on a commercial train (a) maximum traction characteristic and (b) maximum braking characteristic

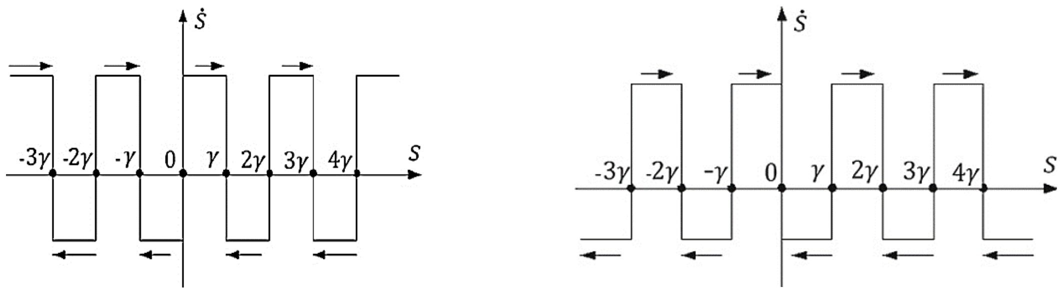

Figure 6. Changes in S and $\dot{S}$ with γ constant: (a) for $dF_x(\kappa)/d\kappa > 0$, and (b) for $dF_x(\kappa)/d\kappa < 0$

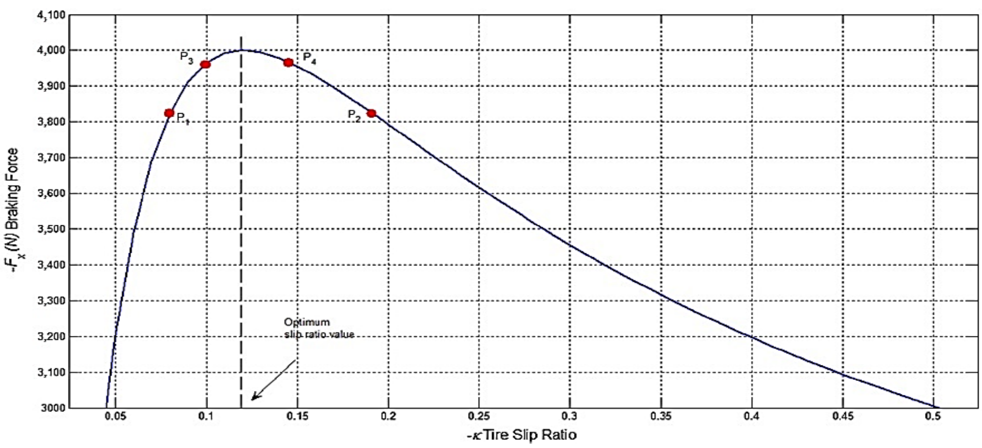

Figure 7. Representative points where ABS works

3.3. Hydraulic braking

EVs also adopted a blended braking system. It contained a hydraulic system as the driving force to obtain a more optimal braking process. The control for the system also used the extended Kalman filter algorithm to make the powertrain more flexible [29]. Regenerative braking plus a hydraulic is usually used on trucks with hydraulic carriers. The regenerative breaking results stored in the battery were used to drive the hydraulic arm.

3.4. Clutch

EVs still use a dual-clutch transmission (DCT), although usually only on conventional vehicles because it has high efficiency and a compact structure. It can also eliminate the need for a torque converter if it uses two clutches simultaneously. Also, it can significantly improve ride comfort, utilize full motor power, reduce engine idling, and optimize engine operating points [30]. In addition, a combined DCT was also developed with a control algorithm for efficient shifting and launching. Figure 8 illustrates the clutch used. The centrifugal structure ensured that only the braking torque was connected to the ECW.

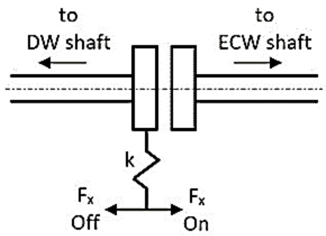

Figure 8. Centrifugal structure in clutch used

4. RESULTS AND DISCUSSION

The study used an induction motor that was gradually loaded. It produced a shaft rotation starting at 500 rpm and increasing by 250 rpm until it reached a maximum rotation of about 2250 rpm. Disc brakes were applied to the DW using conventional hydraulic brakes and ABS. Pressure on the brake piston was set at 2 kg/mm^2. ABS was controlled using a module included in the electronic control unit (ECU). This control was modified using an MBA, in which the frequency on the ABS increased from 10 Hz to 50 Hz. This increase resulted in the replacement of the microcontroller for each frequency. The results are presented in Figure 9.

The speed ratio between ECW and DW was 2. It was applied to make the generator rotate faster and produced a higher electric current. ABS provided a longer wheel stop time than hydraulics. The safety factor in ABS, which avoids wheel locking, caused this time extension. However, the driver can still control the vehicle with actuators [31]. There is a relationship between braking force and wheel slip ratio in ABS [32], as shown in Figure 3.

Hydraulic braking had the shortest time to stop the wheels. It was due to the mechanism that immediately grips the wheel and did not release it at all. This mechanism created the highest friction, and the wheel converted its kinetic energy into heat quickly. This sudden change would affect the induced current of the generator and the torque of the shaft that rotated it. Furthermore, hydraulics is used in heavy vehicles because of their strength [33].

Increasing the frequency of ABS shortened braking time. The periodic graph interval caused the friction intensity to escalate and made the ABS graph close to the hydraulic graph. An increase in ABS frequency brought ABS closer to hydraulics of stopping the wheel. However, ABS provides more safety and maneuverability at high speeds [34]. The power calculation on the generator is presented in Figure 10.

The highest magnetic flux through the generator was achieved by hydraulics. The change in hydraulic induced emf based on (2) was the fastest because it had the shortest braking time. It caused the highest induced current to flow into the battery. The highest power produced the tallest torque, according to (1), and the highest performance. Torque calculation is shown in Figure 11.

Torque depended on ECW shaft power. The generator connected to the ECW was up to 250 W of power, as shown in Table 2. The highest generator power in hydraulic braking ranged from 30 to 50 W, as presented in Figure 10, indicating that the efficiency was 12 to 21%. Graphs in Figure 11 were the shaft torque that rotated the generator and were the torque available in the regenerative braking process.

Different phenomena occurred in energy graphs, as indicated in Figure 12. 10 Hz ABS had the highest energy in harvesting energy during regenerative braking. It had the longest time stopping the wheel and produced the most electricity accumulated in the battery. The longest time indicated that the kinetic energy of the wheel rotation turned into electrical instead of being lost to heat due to friction.

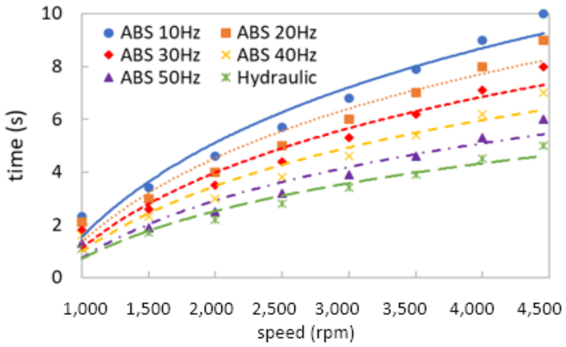

Figure 9. Time braking measurement

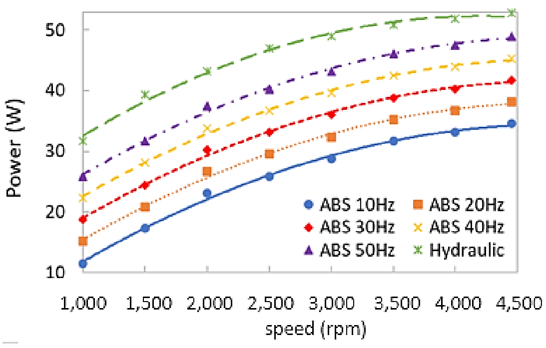

Figure 10. Power on generator

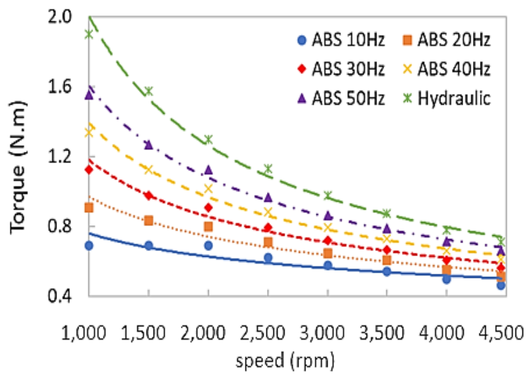

Figure 11. Torque on ECW

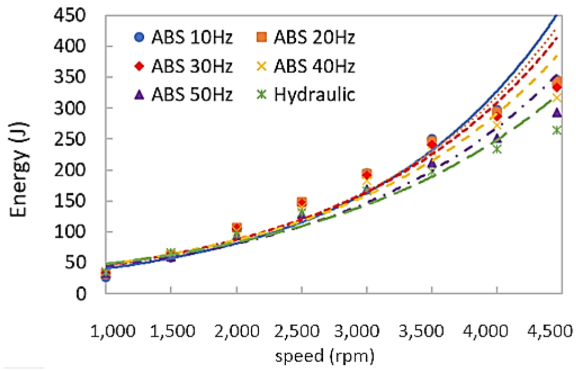

Figure 12. Energy on battery

The 10 Hz ABS had the lowest energy stored in the battery at low revolutions, as shown in Figure 10. It was due to the insignificant time difference in the braking power. Harvesting energy at low speed was dominated by generator power, while wheel stop time took over at high-speed.

No less important than the battery was the cooling system [19]. There was a relationship between electric current and battery temperature. The higher the electricity, the higher the battery temperature [20]. Figure 13 shows the results of measuring battery temperature during harvesting energy from regenerative braking. The hydraulics gave the battery the highest temperature because it had the highest current.

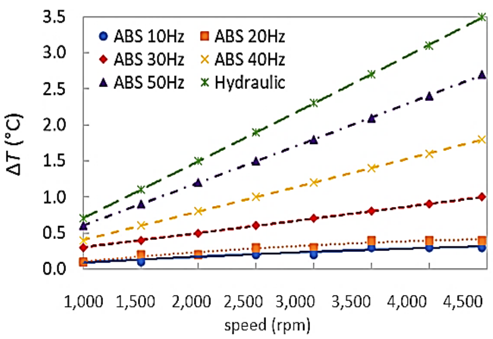

Figure 13. Battery temperature

5. CONCLUSION

EVs offer a solution for saving fossil fuels and preventing environmental damage. In addition, conventional vehicles have lower efficiency in power usage than EVs. EVs can recover energy in several ways, one of which is regenerative braking. The braking system used for regenerative braking is similar to conventional vehicles, with hydraulic brakes and ABS. ABS has a module that contains an algorithm to control the friction between brake and wheel and makes it safer than hydraulic brakes.

The long wheel-stopping time of ABS prevented the wheels from slipping during the braking process. It resulted in the highest harvesting energy in ABS because it allowed a lot of the kinetic energy of wheel rotation to be converted into electricity. However, the generator power in ABS was low because of the low induced current. Lowly potency was advantageous because it did not cause the battery to heat up quickly.

REFERENCES

[1] Y. Zhang, W. Wang, C. Xiang, C. Yang, H. Peng, and C. Wei, "A swarm intelligence-based predictive regenerative braking control strategy for hybrid electric vehicle," *Vehicle System Dynamics*, vol. 60, no. 3, pp. 973–997, 2022, doi: 10.1080/00423114.2020.1845387.
[2] N. Bosso, M. Magelli, and N. Zampieri, "Application of low-power energy harvesting solutions in the railway field: a review," *Vehicle System Dynamics*, vol. 59, no. 6, pp. 841–871, 2021, doi: 10.1080/00423114.2020.1726973.
[3] K. V. Subramaniyam and S. C. Subramanian, "Impact of regenerative braking torque blend-out characteristics on electrified heavy road vehicle braking performance," *Vehicle System Dynamics*, vol. 59, no. 2, pp. 269–294, 2021, doi: 10.1080/00423114.2019.1677921.
[4] E. Katsuyama, M. Yamakado, and M. Abe, "A state-of-the-art review: toward a novel vehicle dynamics control concept taking the driveline of electric vehicles into account as promising control actuators," *Vehicle System Dynamics*, vol. 59, no. 7, pp. 976–1025, 2021, doi: 10.1080/00423114.2021.1916048.
[5] A. Challa, K. Ramakrushnan, P. V. Gaurkar, S. C. Subramanian, G. Vivekanandan, and S. Sivaram, "A 3-phase combined wheel slip and acceleration threshold algorithm for anti-lock braking in heavy commercial road vehicles," *Vehicle System Dynamics*, vol. 60, no. 7, pp. 2312–2333, 2022, doi: 10.1080/00423114.2021.1903048.
[6] L. Castellazzi, A. Tonoli, N. Amati, and E. Galliera, "A study on the role of powertrain system dynamics on vehicle driveability," *Vehicle System Dynamics*, vol. 55, no. 7, pp. 1012–1028, 2017, doi: 10.1080/00423114.2017.1294699.
[7] M. Comellas, J. Pijuan, M. Nogués, and J. Roca, "Efficiency analysis of a multiple axle vehicle with hydrostatic transmission overcoming obstacles," *Vehicle System Dynamics*, vol. 56, no. 1, pp. 55–77, 2018, doi: 10.1080/00423114.2017.1343954.
[8] Z. Hadas, L. Janak, and J. Smilek, "Virtual prototypes of energy harvesting systems for industrial applications," *Mechanical Systems and Signal Processing*, vol. 110, pp. 152–164, 2018, doi: 10.1016/j.ymssp.2018.03.036.
[9] F. Ji, Y. Pan, Y. Zhou, F. Du, Q. Zhang, and G. Li, "Energy recovery based on pedal situation for regenerative braking system of electric vehicle," *Vehicle System Dynamics*, vol. 58, no. 1, pp. 144–173, 2020, doi: 10.1080/00423114.2019.1567927.
[10] C. Pan, L. Chen, L. Chen, H. Jiang, Z. Li, and S. Wang, "Research on motor rotational speed measurement in regenerative braking system of electric vehicle," *Mechanical Systems and Signal Processing*, vol. 66–67, pp. 829–839, 2016, doi: 10.1016/j.ymssp.2015.06.001.
[11] L. Li, X. Li, X. Wang, Y. Liu, J. Song, and X. Ran, "Transient switching control strategy from regenerative braking to anti-lock braking with a semi-brake-by-wire system," *Vehicle System Dynamics*, vol. 54, no. 2, pp. 257–283, 2016, doi: 10.1080/00423114.2015.1129059.
[12] Y. Shi, B. Li, J. Luo, and F. Yu, "A practical identifier design of road variations for anti-lock brake system," *Vehicle System Dynamics*, vol. 57, no. 3, pp. 336–368, 2019, doi: 10.1080/00423114.2018.1467018.
[13] M. Vignati and E. Sabbioni, "Force-based braking control algorithm for vehicles with electric motors," *Vehicle System Dynamics*, vol. 58, no. 9, pp. 1348–1366, 2020, doi: 10.1080/00423114.2019.1621354.
[14] Z. G. Zhao, L. J. Zhou, J. T. Zhang, Q. Zhu, and J. K. Hedrick, "Distributed and self-adaptive vehicle speed estimation in the composite braking case for four-wheel drive hybrid electric car," *Vehicle System Dynamics*, vol. 55, no. 5, pp. 750–773, 2017, doi: 10.1080/00423114.2017.1279739.
[15] M. U. Cuma, Ç. D. Ünal, and M. M. Savrun, "Design and implementation of algorithms for one pedal driving in electric buses," *Engineering Science and Technology, an International Journal*, vol. 24, no. 1, pp. 138–144, 2021, doi: 10.1016/j.jestch.2020.12.014.
[16] Z. Zhou and M. Huang, "Regenerative braking algorithm for the electric vehicle with a seamless two-speed transmission," *Proceedings of the Institution of Mechanical Engineers, Part D: Journal of Automobile Engineering*, vol. 233, no. 4, pp. 905–916, 2019, doi: 10.1177/0954407018755818.
[17] X. Kong, C. Chen, and B. Wen, "Composite synchronization of three eccentric rotors driven by induction motors in a vibrating system," *Mechanical Systems and Signal Processing*, vol. 102, pp. 158–179, 2018, doi: 10.1016/j.ymssp.2017.09.025.
[18] Z. Liu, H. Xiao, P. Khatri, S. Ding, and X. Wang, "A study of a flux switching linear generator with a novel speed amplified mechanism and its optimization for the maximum power output and minimum cogging force of wave energy conversion," *Mechanical Systems and Signal Processing*, vol. 166, 2022, doi: 10.1016/j.ymssp.2021.108413.
[19] T. Sedlacek, D. Odenthal, and D. Wollherr, "Minimum-time optimal control for battery electric vehicles with four wheel-independent drives considering electrical overloading," *Vehicle System Dynamics*, vol. 60, no. 2, pp. 491–515, 2022, doi: 10.1080/00423114.2020.1823004.
[20] X. Hu, C. M. Martinez, and Y. Yang, "Charging, power management, and battery degradation mitigation in plug-in hybrid electric vehicles: A unified cost-optimal approach," *Mechanical Systems and Signal Processing*, vol. 87, pp. 4–16, 2017, doi: 10.1016/j.ymssp.2016.03.004.
[21] V. Krishna Teja Mantripragada and R. Krishna Kumar, "Sensitivity analysis of tyre characteristic parameters on ABS performance," *Vehicle System Dynamics*, vol. 60, no. 1, pp. 47–72, 2022, doi: 10.1080/00423114.2020.1802491.
[22] E. Dinçmen and T. Altınel, "An emergency braking controller based on extremum seeking with experimental implementation," *International Journal of Dynamics and Control*, vol. 6, no. 1, pp. 270–283, 2018, doi: 10.1007/s40435-016-0286-2.
[23] V. Vodovozov, Z. Raud, and E. Petlenkov, "Review on braking energy management in electric vehicles," *Energies*, vol. 14, no. 15, 2021, doi: 10.3390/en14154477.

[24] V. Vodovozov, A. Aksjonov, E. Petlenkov, and Z. Raud, "Neural network-based model reference control of braking electric vehicles," *Energies*, vol. 14, no. 9, 2021, doi: 10.3390/en14092373.

[25] B. Danquah, S. Riedmaier, Y. Meral, and M. Lienkamp, "Statistical Validation Framework for Automotive Vehicle Simulations Using Uncertainty Learning," *Applied Sciences*, vol. 11, no. 5, p. 1983, 2021, doi: 10.3390/app11051983.

[26] A. T. H. T. Anh, N. Van Quyen, N. T. Hai, N. Van Lien, and V. H. Phuong, "Speed profile optimization of an electrified train in cat linh-ha dong metro line based on pontryagin's maximum principle," *International Journal of Electrical and Computer Engineering*, vol. 10, no. 1, pp. 233–242, 2020, doi: 10.11591/ijece.v10i1.pp233-242.

[27] R. Palanisamy, R. Sahasrabuddhe, M. K. Hiteshkumar, and J. A. Puranik, "A new energy regeneration system for a BLDC motor driven electric vehicle," *International Journal of Electrical and Computer Engineering*, vol. 11, no. 4, pp. 2986–2993, 2021, doi: 10.11591/ijece.v11i4.pp2986-2993.

[28] J. S. V. Siva Kumar and P. Mallikarjunarao, "Lqr control of interleaved double dual boost converter for electrical vehicles and renewable energy conversion," *Indonesian Journal of Electrical Engineering and Computer Science*, vol. 16, no. 3, pp. 1240–1248, 2019, doi: 10.11591/ijeecs.v16.i3.pp1240-1248.

[29] P. G. Anselma and G. Belingardi, "Multi-objective optimal computer-aided engineering of hydraulic brake systems for electrified road vehicles," *Vehicle System Dynamics*, vol. 60, no. 2, pp. 391–412, 2022, doi: 10.1080/00423114.2020.1820048.

[30] Z. Zhao, J. Chen, X. Li, and D. Lei, "Downshift decision and process optimal control of dual clutch transmission for hybrid electric vehicles under rapid braking condition," *Mechanical Systems and Signal Processing*, vol. 116, pp. 943–962, 2019, doi: 10.1016/j.ymssp.2018.07.012.

[31] J. Torinsson, M. Jonasson, D. Yang, and B. Jacobson, "Energy reduction by power loss minimisation through wheel torque allocation in electric vehicles: a simulation-based approach," *Vehicle System Dynamics*, vol. 60, no. 5, pp. 1488–1511, 2022, doi: 10.1080/00423114.2020.1858121.

[32] J. Jerrelind, P. Allen, P. Gruber, M. Berg, and L. Drugge, "Contributions of vehicle dynamics to the energy efficient operation of road and rail vehicles," *Vehicle System Dynamics*, vol. 59, no. 7, pp. 1114–1147, 2021, doi: 10.1080/00423114.2021.1913194.

[33] S. Zhou, P. Walker, Y. Tian, and N. Zhang, "Mode switching analysis and control for a parallel hydraulic hybrid vehicle," *Vehicle System Dynamics*, vol. 59, no. 6, pp. 928–948, 2021, doi: 10.1080/00423114.2020.1737147.

[34] M. Tian, Q. Hu, B. Gao, H. Ding, and H. Chen, "Design and handling dynamic analysis of electric vehicle chassis with yaw direction oscillatable battery pack," *Vehicle System Dynamics*, vol. 60, no. 3, pp. 951–972, 2022, doi: 10.1080/00423114.2020.1841902.

BIOGRAPHIES OF AUTHORS

Agung Prijo Budijono is with Universitas Negeri Surabaya, Surabaya, Indonesia, from 2000 to present. From 2001 to 2003, he got the M.Eng. degree in Mechanical Engineering at Institut Teknologi Sepuluh Nopember in 2004. He received B.Eng. at same university from 1990 to 1995. He became an Assistant Professor in 2010, an Associate Professor in 2016, and now he is studying PhD in Institut Teknologi Sepuluh Nopember. His current research interests include electrical vehicles and its applications such as in bicycle and motorcycle. He has published more than 83 journal papers in the fields of mechatronics and its applications. He also has 20 patents. He can be contacted at email: agungbudijono@unesa.ac.id.

I Nyoman Sutantra is a lecturer in Mechanical Engineering Department at the Institut Teknologi Sepuluh Nopember (ITS), Surabaya, Indonesia. He received his B.Eng. degree in Mechanical Engineering from Institut Teknologi Sepuluh Nopember, in 1977. He got M.Sc. degree from University of Wisconsin, Madison, USA in 1980 and Ph.D. degree at same university in 1984. He has been a Professor in ITS, Surabaya, Indonesia since 2003. He is currently Head of Automotive Laboratory ITS. His research interests include the field of Mechanical design, industrial applications, industrial electronics, industrial automotives, vehicles control, etc. He can be contacted at email: sutantra@me.its.ac.id.

Agus Sigit Pramono is a lecturer in Mechanical Engineering Department, Institut Teknologi Sepuluh Nopember (ITS), Surabaya, Indonesia since 1991; and he has been a senior lecturer since 2005. He received the B.Eng. degree in mechanical engineering from Institut Teknologi Sepuluh Nopember, Surabaya, Indonesia, in 1989. He got D.E.A degree from Ecole National Superiure De Aeronatique, France in 1996 and Dr. degree from Universite Paul Sabatier Toulouse III, France in 1999. He is Head of Design System Laboratory ITS. His research interests include the field of design systems, motor drives, industrial applications, industrial electronics, mechatronics. He can be contacted at email: pramono@me.its.ac.id.